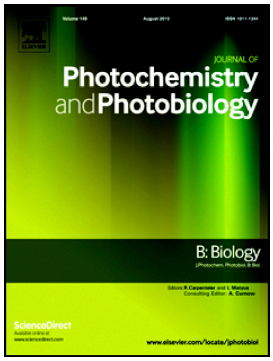

Determination of membrane disruption and genomic DNA binding of cinnamaldehyde to Escherichia coli by use of microbiological and spectroscopic techniques

Tian-Fu He, Zhi-Hong Zhang, Xin-An Zeng, Lang-Hong Wang, Charles S. Brennan

PII: S1011-1344(17)30662-0
DOI: doi:10.1016/j.jphotobiol.2017.11.015
Reference: JPB 11057

To appear in: *Journal of Photochemistry & Photobiology, B: Biology*

Received date: 19 May 2017
Revised date: 25 September 2017
Accepted date: 9 November 2017

Please cite this article as: Tian-Fu He, Zhi-Hong Zhang, Xin-An Zeng, Lang-Hong Wang, Charles S. Brennan , Determination of membrane disruption and genomic DNA binding of cinnamaldehyde to Escherichia coli by use of microbiological and spectroscopic techniques. The address for the corresponding author was captured as affiliation for all authors. Please check if appropriate. Jpb(2017), doi:10.1016/j.jphotobiol.2017.11.015

Determination of membrane disruption and genomic DNA binding of cinnamaldehyde to *Escherichia coli* by use of microbiological and spectroscopic techniques

Tian-Fu He[ab], Zhi-Hong Zhang[ab], Xin-An Zeng[ab]*, Lang-Hong Wang[ab] , Charles S. Brennan[c]

[a] School of Food Sciences and Engineering, South China University of Technology, Guangzhou 510641, China

[b] Food Green Processing and Nutrition Regulation Research Center of Guangdong Province

[c] Department of Wine, Food and Molecular Biosciences, Lincoln University, Lincoln, Canterbury, New Zealand

*Corresponding author. Tel: +86 2087113668, Fax: +86-2039381191. *E-mail address*: xazeng@scut.edu.cn (Prof. Xin-An Zeng);

ABSTRACT

This work was aimed to investigate the antibacterial action of cinnamaldehyde (CIN) against *Escherichia coli* ATCC 8735 (*E. coli*) based on membrane fatty acid composition analysis, alterations of permeability and cell morphology as well as interaction with genomic DNA. Analysis of membrane fatty acids using gas chromatography-mass spectrometry (GC-MS) revealed that the proportion of unsaturated fatty acids (UFA) and saturated fatty acids (SFA) were the major fatty acids in plasmic membrane, and their levels were significantly changed after exposure of *E. coli* to CIN at low concentrations. For example, the proportion of UFA decreased from 39.97% to 20.98%, while the relative content of SFA increased from 50.14% to 67.80% as *E. coli* was grown in increasing concentrations of CIN (from 0 to 0.88 mM). Scanning electron microscopy (SEM) showed that the morphology of *E. coli* cells to be wrinkled, distorted and even lysed after exposure to CIN, which therefore decreased the cell viability. The binding of CIN to genomic DNA was probed using fluorescence, UV−visible absorption spectra, circular dichroism, molecular modeling and atomic force microscopy (AFM). Results indicated that CIN likely bound to the minor groove of genomic DNA, and changed the secondary structure and morphology of this biomacromolecule. Therefore, CIN can be deem as a kind of natural antimicrobial agents, which influence both cell membrane and genomic DNA.

***Keywords*:** Cinnamaldehyde; *Escherichia coli*; Membrane fatty acid; Genomic DNA

1. Introduction

Food-borne pathogens, including *Escherichia coli*, *Staphylococcus aureus*, *Listeria monocytogenes*, *Salmonella typhimurium* induce a large number of serious diseases all over the world [1]. Food processing techniques may increase the risk of microbial cross-contamination of raw materials, thus the prevention of proliferation of pathogenic microorganisms has become an increasingly important issue in food production [2]. Consequently, close attention has been paid to the use of food preservatives with the aim of decreasing nutritional losses due to deleterious microbiological or chemical changes of foods, and thus prolonging shelf life. Safety concerns around the consumption of synthetic substances have attracted attention due to the potential toxicity of these substances. In recent years, people have stressed the importance of natural antimicrobials, which are generally extracted from plants and can not only prevent the growth of foodborne pathogens and spoilage microorganisms, but also enhance the flavor and quality of foods [3].

Researchers have shown that essential oils from *thyme*, *cinnamon bark*, and *lemongrass* have strong antibacterial effects and are generally safe while being added to human food as food additives [4]. Cinnamaldehyde (CIN), a natural ingredient, was first isolated from cinnamon essential oils and was mainly used to impart fragrance to perfumes, food and medical products [5]. CIN has a strong antimicrobial activity, which means that CIN can suppress the growth reproduction of food borne pathogens and spoilage microorganisms [6-7]. Previous research also revealed that the cell membrane integrity, membrane permeability and bacteria morphology may be

damaged when *E. coli* cells are exposed to CIN [8]. Several reports have illustrated that CIN may change structure and function of cell gene in order to restrict the growth of *E. coli* [9]. Although plenty of relevant research has been carried out, the specific sterilization mechanism of CIN is still lacking, which limits the application of CIN. Therefore, the purpose of this work was to provide an overview of the antimicrobial mechanisms of CIN, including the alteration of membrane fatty acid compositions, and damage to cells membrane. This work provides new information regarding the model of the interaction between CIN and DNA by using multi-spectroscopy technology and DNA docking. Such research shows that they do indeed interact and possible target positions. Overall, this work utilized several relevant research methods to explore the antimicrobial mechanism of CIN, so that the result can provide useful suggestions for relevant applications in the future.

2. Materials and methods

2.1. Reagents, strains and incubation conditions

CIN (purity, 99.0%) was purchased from Aladdin Chemistry Co, Ltd. (Shanghai, China). It was prepared under sterile conditions by dissolution in ethanol to a concentration of 5.0 g/L, then was stored at 4 °C. *E. coli* ATCC 8735 provided by Microbial Culture Collection Center of Guangdong Institute of Microbiology (Guangzhou, China) was activated by inoculating thawed stock suspensions into tryptone soy agar supplement with 0.6% yeast extract, which was incubated at 37 °C for 18 to 24 h. Subsequently, a single colony was inoculated to a sterile tryptic soy broth with 0.6% of yeast extraction and incubated at 37 °C for 12 h with shaking at

120 rpm by an orbital shaker (HY-5, JinBo Equipment Industry Co., Jiangsu, China). The activated *E. coli* cells were then transferred to a fresh TSA-YE liquid medium (100 mL, $OD_{600} \approx 0.09$), and cultivated at 37 °C with shaking at 120 r/min with equal volumes of ethanol (0.52%, control) and CIN at final concentrations of 0.29mM, 0.59mM and 0.88mM, respectively. The cells were cultivated at 37 °C on a rotary shaker at 120 rpm with different concentration of CIN as above until the mid-stationary phase was achieved, and the optical density of culture was about 1.60. After inoculation, these cultures were placed in each of four sterilized, 50 mL plastic screw-cap centrifuge tubes and then centrifuged at 4000 × *g* for 5 min at 4 °C in a refrigerated centrifuge (JW-3021HR, Anhui Jiaven Equipment Industry Co., Anqing, China). After removing the supernatants, the four pellets were washed twice with sterile water separately and prepared for analysis of their membrane fatty acid composition.

2.2 Analysis of membrane fatty acid composition

The cultures of *E. coli* ($OD_{600} \approx 1.6$) were centrifuged at 4000 × *g* for 5 min at 4 °C in a refrigerated centrifuge (JW-3021HR, Anhui Jiaven Equipment Industry Co., Anqing, China), then fresh pellets were obtained, which were used for extraction of membrane fatty acids. Fatty acids of the cell membrane were extracted according to previous studies [10-11]. Firstly, 40 mg of fresh pellets, 1.0 mL saponification solution (4.5 g NaOH, 15.0 mL methanol, and 15.0 mL distilled water) and 2.0 mL methylation solution (32.5 mL of 6.0 M HCl and 27.5 mL of methanol) were added into a 10 mL tube, after mixing for a few seconds 1.25 mL extraction mixture solution

(hexane and methyl-tert-butyl ether, v/v=1:1) was added and followed by the addition 3.0 mL of 0.3 M NaOH. Finally, two thirds of the organic phase was separated for GC-MS analysis. Analysis of fatty acid methyl esters were performed on a GC Agilent 7820A (Agilent Technologies, Wilmington, DE, USA) equipped with a capillary column HP-5 (30 m × 0.32 mm × 0.25 μm, Agilent Technologies, Wilmington, DE, USA) using pure nitrogen as carrier gas at 1.0 mL/min in a split mode (20:1). After relevant calculations and graphics processing, the final results were expressed as figures containing the relative content of different kinds of each fatty acid and the proportion of a fatty acid to another.

2.3 Scanning electron microscopy

The morphological observation of *E. coli* cells were carried out by scanning electron microscopy (SEM, Zeiss EVO18, Germany) using a procedure described in a previous study [12]. *E. coli* cells were fixed in glutaraldehyde (2.5% in 0.01 M phosphate buffer, pH 7.2) overnight at 4 °C. After centrifugation at 4000 × *g* for 5 min at 4 °C (JW-3021HR, Anhui Jiaven Equipment Industry Co., Anqing, China), the cells were washed by 0.01 M phosphate buffer twice, and then dehydrated using a gradient of different ethanol solutions (30%, 50%, 70%, 80%, 90%, 95% and 100%; 30 min each time). Afterwards, the cells were incubated in tertiary-butanol twice for 30 min, and placed on a silicon wafer prior to vacuum freeze drying (Hitachi ES-2030). Finally, the cells were mounted on aluminum stubs with double-sided sticky conductive metal tape, and gold-coated using ion sputter (Jeol JFC1100, Japan), which was operated at 10.0 kV.

2.4 Effects of CIN on genomic DNA

The genomic DNA of *E. coli* cells was extracted by a GenElute bacterial genomic DNA kit (Sigma−Aldrich), the purity of the DNA was confirmed by the ratio of A_{260}/A_{280} > 1.80, then the extracted DNA was dissolved in a TE solution (10 mM Tris−HCl, 0.1 mM EDTA; pH 8.0) at a final concentration of 1.92 mM, as measured by UV absorption at 260 nm using a molar absorption coefficient ε260 = 6600 M^{-1} cm^{-1}. The interaction between CIN and genomic DNA of *E. coli* was investigated by fluorescence (Hitachi Model F–7000 spectrofluorimeter, Japan), UV-Vis absorption spectra (UV-1800, Shimadzu, Japan) and a Bio-Logic MOS 450 circular dichroism spectrometer (Bio-Logic, Claix, France). All tests were carried out three times.

2.5 Molecular simulation

The studies of molecular docking of CIN with DNA were performed by AutoDock software with the aid of the MGL tools 1.5.6rc3 according to a previous report [13]. Before modeling the docking, the relevant crystal structure of the B-DNA was downloaded from the Protein Data Bank (ID: 5LCV), and polar hydrogen atoms and Gasteiger charges were added to the macromolecule file, which could help to optimize the model of DNA. The structure of CIN was formed by using Sybyl-x 2.0 and was optimized to minimal energy by using Gasteiger-Huckel charges. Afterwards, the CIN molecule was allowed to move over the structure of DNA with 100 runs to discover the possible binding positions. As the position of CIN–DNA with the lowest energy was discovered, it could be inferred that this position was the most possible

place where CIN–DNA interact.

2.6 Atomic force microscope

Atomic force microscope (AFM), one of the near-field microscopes, which can investigate surfaces of samples on an atomic scale without any damage, is widely used in structure – function research [14-15]. In this work, a Multimode 8 SPM AFM (Bruker, Karlsruhe, Germany) in tapping mode was used to observe the morphology of DNA of the cells in absence and presence of CIN (0, 2.0 mM). Its SCANASYST-AIR probes have a normal spring constant and tip radius of 0.4 N/m and 2 nm, respectively. In order to ensure the consistency of figure height, the peak force was set to 2.5 nN for all samples. The samples of 10 μL of mixed solution in absence and presence of CIN contained 0.5 mM DNA and after incubation for 3 hours at room temperature, 5 μL of these samples were dropped onto polished silicon wafers, and air dried overnight. Then, they were imaged by intelligent scanning mode and processed with the Nanoscope Analysis v150r1sr3 software package.

3. Results and discussion

3.1 Effect of CIN on membrane fatty acid composition of E. coli

Previous research had suggested that the minimum inhibitory concentration (MIC) of CIN toward *E. coli* was 0.31 g/L (2.35 mM) [8]. Our work reports the influence of CIN on the cell membrane by changing its concentration (0, 0.29 mM (1/8 MIC), 0.59 mM (1/4 MIC) and 0.88 mM (3/8 MIC)). As shown in Table. 1, Fig. 1, 13 kinds of fatty acids compositions were detected, they were respectively called lauric acid (C12:0), tetradecanoic acid (C14:0), 2-hydroxytetradecanoic acid (2-OH

C14:0), 3-hydroxytetradecanoic acid (3-OH C14:0), palmitoleic acid (C16:1ω9), hexadecanoic acid (C16:0), (C17:Cyclo), (C17:1ω10), heptadecane acid (C17:0), (C18:1ω9), octadecane (C18:0), (C19:Cyclo), nonadecane acid (C19:0). The fatty acids could be roughly divided into two categories, saturated fatty acids (SFA) (including C12:0, C14:0, C16:0, C17:0, C18:0, C19:0) and unsaturated fatty acids (UFA) (including C16:1ω9, C17:1ω10, C18:1ω9). Among all kinds of fatty acids composition, C14:0, C16:1ω9, C16:0, C17:1ω10, C18:1ω9 were dominant, and they occupied 9.81%, 10.98%, 32.68%, 18.4% and 10.59%, respectively, which could be seen from Fig.1A. The effect of increasing the concentration of CIN was to decrease UFA content, while SFA content increased as shown in Fig.1B. For instance, when CIN was absent, the UFA content was 39.97%, and the SFA content was 50.14%, respectively. As *E. coli* cells were exposed to CIN at 0.88mM, the content of UFA gradually decreased to 20.98% and SFA content gradually increased to 67.8%. Moreover, it could be inferred that the majority of the increase of the SFA was due to the increase of C14:0, C16:0, C18:0. The proportions of C14:0, C16:0, C18:0 increased from 9.81%, 32.68% and 3.4% to 17.55%, 38.47% and 7.35%, respectively, when the concentration of CIN increased from 0 to 0.88mM, whereas the decrease of C16:1ω9, C17:1ω10 and C18:1ω9 mainly led to the UFA content decreasing. The contents of C16:1ω9, C17:1ω10 and C18:1ω9 decreased from 10.98%, 18.4% and 10.59% to 3.86%, 12.59% and 4.53%, respectively, when *E. coli* was grown in increasing concentration of CIN (from 0 to 0.88 mM). Furthermore, SFA/UFA increased from 1.25 to 3.23 with the concentration of CIN increasing as shown in

Fig.1C.

Previous studies have confirmed that the microorganism tries to adapt to the change of environment by adjusting the proportion of SFA to UFA, which meant that the fluidity of the membrane changed, in order to protect itself [16-17]. For example, the membrane fluidity of *S. aureus* changed when the cells were incubated at a high temperature. The proportion of SFA to UFA increased in order to lessen damage [13]. The proportion of SFA in the membrane of *E. coli* cells gradually increased with the concentration of phenol increasing, which is a reaction that helps the organism to resist the harm of antibacterial substances [18]. The compositions of membrane fatty acids were observed to change when methanolic solutions of thymol, carvacrol, limonene, Cinnamaldehyde, and eugenol were added into growth media of *Salmonella enterica serovar typhimurium* and *S. aureus* strains [19]. Previous studies have explained that the spatial structure of SFA is relatively larger than the spatial structure of UFA, so when the proportion of SFA to UFA was increased, fluidity of *E. coli* decreased, which helped to resist adverse changes in the external environment [17]. It can be seen from Fig.1C that, with increasing concentration of CIN the proportion of SFA to UFA also increased. Therefore, the figures showed that the fluidity of *E. coli* was decreased when the cells were incubated in a high concentration of CIN. Moreover it could be inferred that when the concentration of the CIN changed, the *E. coli* cells were prone to process replacement of the fatty acids. This change in membrane structure and function may be attributed to self-protection a process which potentially occurred in order to try to resist the toxic stress induced by CIN.

3.2 Morphological observations of E. coli cells

The morphology of cells treated in different concentration of CIN (0, 0.5 MIC, 1.0 MIC, 2.0 MIC) can be seen in Fig. 2. As shown in Fig. 2A, the untreated cells maintained their original structure and exhibited normal smooth surface. When cultured in 0.5 MIC CIN, cells became rough and wrinkled (Fig. 2B). In addition, the *E. coli* incubated in 1.0 MIC CIN were distorted in original shape and some cells even collapsed, which can be seen in Fig. 2C. At 2 MIC CIN (Fig. 2D), most of the cells dissolved and couldn't be distinguished easily. These figures revealed that CIN played a significant role in morphology of treated *E. coli* and as the concentration of CIN increased, the damage of CIN to the integrity of *E. coli* cell membrane became more and more serious. Previous studies indicated that lipophilic properties can help cell membrane penetration and under stressed conditions may rupture the bacterial cell [20]. The data from SEM agreed with this view because CIN has a high lipophilic distribution coefficient and actually destroyed the structure of cell membrane. It was reported that the structures of *Escherichia coli* O157:H7, *Staphylococcus aureus, Salmonella enterica serovar; Typhimurium Pseudomonas fluorescens, and Brochothrix thermosphacta* cells were changed after being cultured in media added with thymol, carvacrol, limonene, eugenol, and cinnamaldehyde. The SEM images suggested that these natural antibacterial substances had anti-bacteria abilities that influenced membrane integrities [19]. In short, the observation demonstrated that CIN has significant effect on the structure of cell membrane and can make it rough, wrinkled, distorted, collapsed and even rupture depending on concentration.

3.3 The interaction of CIN with DNA

Many antimicrobials can not only destroy cell membrane, but also have impacts on other structures, such as DNA, RNA and so on [21]. Therefore, in order to detect whether CIN is able to interact with DNA, research was carried out using fluorescence techniques [22-23]. As shown in Fig 3A, CIN had a strong fluorescence mission peak at 309 nm when its λ_{ex} was 270 nm. As the concentration of DNA increased, fluorescence intensity of CIN had an obvious reduction. This kind of wave pattern indicates that CIN can interact with DNA [24]. Zhang et al had put forward a modified equation to describe the connection between CIN and DNA, which directly helps to explain their combing and determine the binding constant (*K*) [24].

$$\frac{F_0}{F_0 - F} = \frac{1}{f_a K_a} \frac{1}{[\mathrm{DNA}]} + \frac{1}{f_a}$$

where F_0 and F represents the fluorescence intensity of CIN in absence and presence of DNA, respectively. Additionally, f_a is the fraction of accessible fluorescence and [DNA] denotes the concentration of DNA. As shown in Fig. 3B, the ratio of intercept to the slope can be used to calculate the value of binding constant K and it was estimated to be $(2.61 \pm 0.13) \times 10^4\ \mathrm{M}^{-1}$ (R^2 = 0.9997). Previous studies discovered that the values of the binding constant, *K*, of ethidium bromide and acridine orange, which can be seen as classical indicators with DNA, were $2.6 \times 10^6\ \mathrm{M}^{-1}$ and $4.0 \times 10^5\ \mathrm{M}^{-1}$, respectively [25]. These values were both higher than the *K* value obtained here. However, the *K* value of the substances binding with DNA via grooves was roughly similar to this value [26]. Therefore, it can be inferred that CIN may also interact with DNA in the grooves.

In this work, UV absorption spectroscopy was used to analyze the significant affects of CIN on DNA. Fig 3C was obtained by subtracting the absorbing spectra of free DNA from complex, showing that the absorbance of CIN exhibits an obvious maximum at 309 nm and reduces mildly, without a shift, with the increase of concentration of DNA. The results further suggest that there was a groove binding mode between CIN and genomic DNA.

Circular dichroism (CD) technique can provide information about the absolute configuration of organic compounds, conformation and reaction mechanism, which is a powerful and useful tool to study the binding between small molecules and DNA [27-28]. As shown in Fig 3D, the negative band at 245 nm showed that this DNA had a right-handed helicity. Additionally, the positive band at around 275 nm corresponded to base stacking, implying that it was a typical B-DNA structure [29]. As the concentration of CIN increased (1.0 to 2.0mM), a slightly gradual decrease shifting can be observed in the negative band, while no apparent change happened in the positive band. Previous studies showed that the intensities of the positive and negative band have no apparent change, when small molecules bind to DNA via minor grooves [30-32] and the wave patterns of our results were consistent with these studies, suggesting that CIN may combine with DNA in the mode of groove binding. It was reported that Citral can suppress the growth of *Aspergillus flavus* because it interacts with DNA, changing the structure of DNA [21]. Hu et al have revealed that CIN influences the structure of *cyanobacteria cell* DNA, leading to the death of microorganism [33]. Therefore, it can be inferred that CIN binds to DNA via minor

grooves, leading to disorders of gene expression, which could be taken as one of the antibacterial mechanisms of CIN.

3.4 Molecule simulation

In order to learn how CIN combines with DNA, a molecular docking technique was used to show an intuitive display of the interaction of CIN with DNA. After successfully processing 100 molecular docking runs, 15 kinds of energy clusters with different frequency of occurrence were ranked and shown in Fig 4A. Among all energy clusters, the cluster with the largest number of conformations (30 out of 100) processed the energy of −3.55 kcal M^{-1}, which is too high for CIN-DNA complex to maintain their structure, while the cluster (blue histogram) with the lowest energy (−5.58 kcal M−1), contained a number of analyzed conformations (9 out of 100) , which is only fewer in number than the cluster with the energy of −3.55 kcal M^{-1} (30 out of 100) and the cluster with the energy of −3.35 kcal M^{-1} (15 out of 100), it is therefore ranked in the third place out of 15 types of cluster. Therefore, the cluster with the lowest energy can be regarded as the one most likely to generate the connection between CIN and DNA, and was selected to use in binding orientation analysis to find the possible position of their combining.

After carrying out relevant molecule simulation, a model of the treated DNA was formed, shown in Fig.4B. In this model, CIN combined with DNA in minor grooves, adenine(A)-thymine(T) rich regions, surrounded by the base pairs of A14, A16, T19, and T20 and they formed complex connection by hydrogen bonding (green dashed lines). The length of the hydrogen bond was nearly 1.866 Å and it connected the

hydrogen atom H21 of the fifth guanine base on the chain B with the oxygen atom of CIN. The result of this docking research implies that CIN interacted with DNA by entering into the minor groove of DNA, and their combination is mainly achieved by hydrogen bonding.

3.5 DNA observation

The observations of DNA are shown in Fig. 5. As shown in Fig. 5A, the appearance of free DNA was smooth and distributed well across the surface of mica. The mean height of untreated individual DNA was approximately 1.5 nm (Fig. 5C). However, the DNA after being treated with CIN (2.0 mM) was prone to be cross-linking and non-regular with a mean height of 3.1 nm (Fig. 5D). These results analyzed by AFM images and CD spectroscopy imply that CIN influenced the structure of the DNA, especially the secondary structure, causing the DNA to aggregate together after treatment with CIN.

4. Discussion

There were 13 kinds of fatty acids compositions identified as the primary fatty acids in the *E. coli* membrane, including lauric acid (C12:0), tetradecanoic acid (C14:0), 2-hydroxytetradecanoic acid (2-OH C14:0), 3-hydroxytetradecanoic acid (3-OH C14:0), palmitoleic acid (C16:1ω9), hexadecanoic acid (C16:0), (C17:Cyclo), (C17:1ω10), heptadecane acid (C17:0), (C18:1ω9), octadecane (C18:0), (C19:Cyclo), nonadecane acid (C19:0) (Table.1 and Fig. 1). It has been reported that the increase of an antibacterial substance concentration induced an increase of SFA and a contrasting reduction of UFA, this adjusts the fluidity of cell membrane allowing the *E. coli* to

enhance their self-protection ability and thus resist adverse changes in the external environment [16-17]. Generally, UFA have a small spatial structure and a low melting point, leading to an increase in membrane fluidity, while SFA have a relatively large structure and a high melting point, which reduces membrane fluidity [17]. Jean-Louis Nano et al have indicated previously that UFA can enhance membrane fluidity, but palmitic acid (a kind of SFA) didn't induce any obvious change [34]. The proportion of SFA to UFA in the *E. coli* cell membrane was increased with the increasing concentration of phenols [18]. An increase of UFA was found in *S. Aureus* membrane after addition of carvarol to the growth medium [35]. Consequently, the CIN sterilization mechanism may be related to cell membrane fluidity. Furthermore, our results were consistent with the images of SEM, which exhibited that the morphology of *E. coli* became wrinkled, distorted and even dissolved (Fig. 2). Therefore, it can be inferred that CIN has significant impacts on cell membrane, by altering its fatty acids compositions to change cell membrane fluidity and surfaces, which can be deemed as one of its sterilization mechanisms.

Apart from the cell membrane, CIN also interacted with DNA via minor grooves by hydrogen bonding, potentially resulting in a disorder of gene expression. DNA spectral information, binding constant, binding mode and DNA structure were used to analyze the combination of CIN and DNA. The images (Fig. 3A, C, D) shown by fluorescence techniques and circular dichroism indicated that CIN might interact with DNA in the grooves, which is similar to previous studies [26, 31]. Besides, the classical binding constant values (K), ethidium bromide ($2.6 \times 10^6\,M^{-1}$) and acridine

orange (4.0×10^5 M^{-1}) [25], were both in the order of 10^5-10^6 M^{-1}, which were significantly higher than the binding constant value (K) in the present study, estimated to be $(2.61 \pm 0.13) \times 10^4$ M^{-1}. However, this obtained K was similar to the K value of groove binders of DNA [26], suggesting that CIN may interact with DNA via grooves. Moreover, a model of the DNA treated by CIN indicated that CIN combined with DNA by entering into the minor grooves. Hydrogen bonds connected hydrogen atom H21 of the fifth guanine base on chain B with the oxygen atom of CIN, implying that the hydrogen bond force played a significant role in their combination. AFM images showed aggregated DNA molecules after being treated with CIN. This result was consistent with a previous study which indicated that DNA changed to be cross-linking and non-regular after interacting with small molecules [28]. According to these above studies, CIN might generate its antibacterial influence by interacting with genomic DNA, and change DNA structure, especially DNA secondary structure, which can be taken as its sterilizing mechanism as well.

Our results revealed that CIN has potential antimicrobial abilities, including alteration and destruction of cell membrane and interaction with genomic DNA. It can be inferred that CIN has important impacts on *E.coli* cell membrane in order to enhance its permeability so that it can enter and spread throughout the interior of the cell. Besides, biological macromolecules within cells such as DNA, might be the CIN targets as well, and CIN destroys the original structure of DNA, significantly interfering gene expression, which effectively leads to cell death.

5. Conclusions

This work mainly investigated the sterilization mechanism of CIN on *Escherichia coli*. The antibacterial effect of CIN could be roughly divided two categories. One was changing the fatty acids composition of *E. coli* membrane and changing the appearance of *E. coli*. The other was interaction with DNA via the minor groove, so that CIN was able to directly impact on the DNA of the treated cells. Analysis of membrane fatty acid compositions and morphological observations indicated that the rate of saturated fatty acids and unsaturated fatty acids would change with the increasing concentration of CIN, which could not only influence the morphology of the cells, but also modify the fluidity of *E. coli*. Besides, relevant in vitro experiments, on the method of Uv-Vis Spectrophotometry, fluorescence and circular dichroism, molecule simulation and atomic force microscope, revealed that CIN actually could play a significant role in DNA and it could be connect with DNA by hydrogen bonds in minor grooves to form CIN-DNA complex, leading to slight changes in DNA secondary structure and surface morphology. In a word, all these analyses showed that CIN has obvious antibacterial influence on *E. coli*, including its cell membrane and DNA, so it could be commonly used in future as an effective preservative in order to enhance the security of food and maintain the natural food at the meantime.

Acknowledgement

This research was supported by the National Natural Science Foundation of China (21576099, 21376094) as well as S&T projects of Guangdong Province (2015A030312001 and 2013B020203001).

References

[1] B. NagyP. Z. Fekete, Enterotoxigenic Escherichia coli (ETEC) in farm animals, Vet Res. 30 (1999) 259.

[2] A. A. Mohamed, S. I. Ali, F. K. EL-Baz, A. K. HegazyM. A. Kord, Chemical composition of essential oil and in vitro antioxidant and antimicrobial activities of crude extracts of Commiphora myrrha resin, Ind Crop Prod. 57 (2014) 10-16.

[3] Perumal, A. B., Sellamuthu, P. S., Nambiar, R. B., Sadiku, E. R., Antifungal activity of five different essential oils in vapour phase for the control of Colletotrichum gloeosporioides and Lasiodiplodia theobromae in vitro and on mango, Int J Food Sci Tech. 51 (2016) 411-418.

[4] Stratakos, A. C., Koidis, A., Suitability, efficiency and microbiological safety of novel physical technologies for the processing of ready- to- eat meals, meats and pumpable products, Int J Food Sci Tech. 50 (2015) 1283-1302.

[5] D. Bickers, P. Calow, H. Greim, J. M. Hanifin, A. E. Rogers, J. H. Saurat, I. G. Sipes, R. L. SmithH. Tagami, A toxicologic and dermatologic assessment of cinnamyl alcohol, cinnamaldehyde and cinnamic acid when used as fragrance ingredients, Food Chem Toxicol. 43 (2005) 799-836.

[6] Wang L H, Wang M S, Zeng X A, An in vitro investigation of the inhibitory mechanism of β-galactosidase by cinnamaldehyde alone and in combination with carvacrol and thymol, Biochimica et Biophysica Acta (BBA) - General Subjects. (2016).

[7] N. Sanla-Ead, A. Jangchud, V. ChonhenchobP. Suppakul, Antimicrobial Activity

of Cinnamaldehyde and Eugenol and Their Activity after Incorporation into Cellulose-based Packaging Films, Packag Technol Sci. 25 (2012) 7-17.

[8] S. Shen, T. Zhang, Y. Yuan, S. Lin, J. XuH. Ye, Effects of cinnamaldehyde on Escherichia coli and Staphylococcus aureus membrane, Food Control. 47 (2015) 196-202.

[9] Mdowell, P., Affas, Z., Reynolds, C., Holden, M. T., Wood, S. J., Saint, S., Structure, activity and evolution of the group i thiolactone peptide quorum-sensing system of staphylococcus aureus, Mol Microbiol. 41 (2001) 503-12.

[10] Sasser, M., Identification of bacteria by gas chromatography of cellular fatty acids (1990).

[11] Schutter, M. E., Dick, R. P., Comparison of fatty acid methyl ester (FAME) methods for characterizing microbial communities, Soil Sci Soc Am J. 64 (2000) 1659-1668.

[12] Wang, L. H., Wang, M. S., Zeng, X. A., Zhang, Z. H., Gong, D. M., Huang, Y. B., Membrane Destruction and DNA Binding of Staphylococcus aureus Cells Induced by Carvacrol and Its Combined Effect with a Pulsed Electric Field, J. Agric. Food Chem. 64 (2016) 6355-6363.

[13] Wang, L., Tao, M., Zhang, G., Li, S., Gong, D., Partial intercalative binding of the food colorant erythrosine to herring sperm DNA, RSC Adv. 5 (2015) 98366-98376.

[14] Radmacher, M., Tillmann, R. W., Fritz, M., Gaub, H. E., From molecules to cells:

imaging soft samples with the atomic force microscope, Science. 257 (1992) 1900-1906.

[15] Binnig, G., Quate, C. F., Gerber, C., Atomic force microscope, Phys Rev Lett. 56 (1986) 930.

[16] Burns, C. P., Luttenegger, D. G., Dudley, D. T., Buettner, G. R., Spector, A. A., Effect of modification of plasma membrane fatty acid composition on fluidity and methotrexate transport in L1210 murine leukemia cells, Cancer Res. 39 (1979) 1726-1732.

[17] T. J. Denich, LA Beaudette, H. LeeJ. T. Trevors, Effect of selected environmental and physico-chemical factors on bacterial cytoplasmic membranes, J Microbiol Methods. 52 (2003) 149-182.

[18] H. Keweloh, R. DiefenbachH. J. Rehm, Increase of phenol tolerance of Escherichia coli by alterations of the fatty acid composition of the membrane lipids, Arch Microbiol. 157 (1991) 49-53.

[19] Di Pasqua, R., Hoskins, N., Betts, G., Mauriello, G., Changes in membrane fatty acids composition of microbial cells induced by addiction of thymol, carvacrol, limonene, cinnamaldehyde, and eugenol in the growing media, JJ. Agric. Food Chem. 54 (2006) 2745-2749.

[20] M. Kong, X. G. Chen, K. XingH. J. Park, Antimicrobial properties of chitosan and mode of action: A state of the art review, Int J Food Microbiol. 144 (2010) 51-63.

[21] Luo, M., Huang, Y., Jiang, L., Ji, T., & Tu, M., Study on quantitative test on the

DNA damage of Aspergillus flavus caused by citral with a comet analysis system, Acta Microbiol Hung. 42 (2002) 341-347.

[22] Y. ZhouY. Li, Studies of interaction between poly(allylamine hydrochloride) and double helix DNA by spectral methods, Biophys Chem. 107 (2004) 273-281.

[23] Nygren, J., Svanvik, N., Kubista, M., The interactions between the fluorescent dye thiazole orange and DNA, Biopolymers. 46 (1998) 39-51.

[24] Zhang, G., Wang, L., Zhou, X., Li, Y., Gong, D., Binding characteristics of sodium saccharin with calf thymus DNA in vitro, J. Agric. Food Chem. 62 (2014) 991-1000.

[25] Hammer, K. A., Heel, K. A., Use of multiparameter flow cytometry to determine the effects of monoterpenoids and phenylpropanoids on membrane polarity and permeability in staphylococci and enterococci, Int J Antimicrob Agents. 40 (2012) 239-245.

[26] W. Kangwansupamonkon, V. Lauruengtana, S. SurassmoU. Ruktanonchai, Antibacterial effect of apatite-coated titanium dioxide for textiles applications, Nanomedicine. 5 (2009) 240-249.

[27] Carvlin, M. J., Mark, E., Fiel, R., Howard, J. C., Intercalative and nonintercalative binding of large cationic porphyrin ligands to polynucleotides, Nucleic Acids Res.11 (1983) 6141-6154.

[28] I. AhmadM. Ahmad, Dacarbazine as a minor groove binder of DNA: Spectroscopic, biophysical and molecular docking studies, Int J Biol Macromol. 79 (2015) 193-200.

[29] Mati, S. S., Roy, S. S., Chall, S., Bhattacharya, S., Bhattacharya, S. C. Unveiling the groove binding mechanism of a biocompatible naphthalimide-based organoselenocyanate with calf thymus DNA: An “ex vivo” fluorescence imaging application appended by biophysical experiments and molecular docking simulations, J Phys Chem B. 117 (2013) 14655-14665.

[30] Liu, Z., Xiang, Q., Du, L., Song, G., Wang, Y., Liu, X., The interaction of sesamol with DNA and cytotoxicity, apoptosis, and localization in HepG2 cells, Food Chem. 141 (2013) 289-296.

[31] M. Tao, G. Zhang, J. PanC. Xiong, Deciphering the groove binding modes of tau-fluvalinate and flumethrin with calf thymus DNA, Spectrochim Acta A. 155 (2016) 28-37.

[32] Wang L H, Zhang Z H, Zeng X A, Erratum to: Combination of microbiological, spectroscopic and molecular docking techniques to study the antibacterial mechanism of thymol against Staphylococcus aureus: membrane damage and genomic DNA binding, Analytical & Bioanalytical Chemistry. 409 (2017) 3055-3055.

[33] L. B. Hu, W. Zhou, J. D. Yang, J. Chen, Y. F. YinZ. Q. Shi, Cinnamaldehyde Induces PCD-Like Death of Microcystis aeruginosa via Reactive Oxygen Species,Water Air Soil Pollut. 217 (2011) 105-113.

[34] J. Nano, C. Nobili, F. Girard-PipauP. Rampal, Effects of fatty acids on the growth of Caco-2 cells, Prostaglandins, Prostaglandins Leukot Essent Fatty Acids. 69 (2003) 207-215.

[35] Wang, L. H., Wang, M. S., Zeng, X. A., Liu, Z. W., Temperature-mediated variations in cellular membrane fatty acid composition of Staphylococcus aureus in resistance to pulsed electric fields, BBA-Biomembranes. 1858 (2016) 1791-1800.

Figure captions

Fig. 1 (A) The relative proportions of different kinds of fatty acid, (B) Relative contents of SFAs and UFAs, and (C) The ratios of SFAs to UFAs with concentrations of CIN increasing. Data were expressed as mean ± standard deviation (N = 3).

Fig. 2 The surface observations of *Escherichia coli* treated in different concentrations of CIN. (A) Control group; (B) 0.5 MIC ; (C) 1.0 MIC ; (D) 2.0 MIC.

Fig. 3 (A) The influence of CIN on DNA showed by fluorescence spectra (T = 298 K, pH 7.4, λ_{ex} = 270 nm, λ_{em} = 309 nm); c(CIN) = 5.08 × 10^{-5} M; and c(DNA) = 0, 0.64, 1.28, 1.92, 2.56, 3.20, 3.84, 4.48, 5.12, and 5.76 × 10^{-5} M, for curves 1→10, respectively; (B) UV difference spectra [(DNA solution + thymol solution)−DNA solution] for CIN with various concentrations of DNA in the wavelength range of 200–350 nm. c(CIN)=2.29 × 10^{-4} M; c(DNA)=0, 1.92, 3.84, 5.76, 7.68, and 9.60 × 10^{-5} M corresponding to the curves from 1→5, respectively; (C) the modified Stern-Volmer plots of CIN by DNA at room temperature; (D) Circular dichroism spectra of DNA with the concentrations of CIN increasing at pH 7.4. c(DNA) = 5.00 × 10^{-4} M. The molar ratios of CIN to DNA were 0:1, 2:1, and 4:1 for curves 1→3, respectively. c(CIN) = 5.00 × 10^{-4} mol L^{-1} (dashed line).

Fig. 4 (A) Cluster analyses of the AutoDock docking runs of CIN with DNA; (B) Molecular modeling structure of CIN–DNA system. And the area marked in blue was the place possessing the lowest binding energy. The area marked in green was hydrogen bonds.

Fig. 5 The observations of appearance of DNA structure. (A) DNA of the untreated

cells;(B) DNA of the treated cells;(C) the height of the DNA of the treated cells;(D) the height of the DNA of the untreated cells. The scan size of the image is 2.0 μm × 2.0 μm, respectively. *c*(DNA) = 0.5 mM and c(CIN) = 2.0 mM.

Table. 1 Total fatty acid composition (%) of *E. coli* membrane at various concentrations of CIN. Each value is the mean of three replicates ± SD. All identified fatty acids had similitude index (SI) of more than 90%.

Fatty acids	Total composition (%) at various concentrations of CIN				
	0	0.125 MIC	0.25 MIC	0.375 MIC	Ethanol (0.52%)
C12:0	1.52 ± 0.52	0.98 ± 0.06	0.94 ± 0.13	0.41 ± 0.09	0.41 ± 0.08
C14:0	9.81 ± 1.03	12.21 ± 0.73	16.38 ± 0.94	17.55 ± 0.9	8.55 ± 0.21
2OH-C14:0	0.19 ± 0.08	0.17 ± 0.01	0.18 ± 0.03	0.26 ± 0.06	0.28 ± 0.02
3OH-C14:0	6.47 ± 0.68	6 ± 0.64	5.45 ± 0.24	7.51 ± 0.85	6.51 ± 0.89
C16:1ω9	10.98 ± 1.05	8.57 ± 0.83	6.92 ± 0.26	3.86 ± 0.96	13.84 ± 1.36
C16:0	32.68 ± 1.83	35.98 ± 2.15	36.51 ± 1.95	38.47 ± 1.84	30.47 ± 2.8
C17:Cyclo	0.6 ± 0.04	0.66 ± 0.08	0.72 ± 0.04	1.1 ± 0.05	1.32 ± 0.05
C17:1ω10	18.4 ± 0.89	18.36 ± 0.63	17.13 ± 0.8	12.59 ± 0.49	20.09 ± 1.19
C17:0	0.55 ± 0.03	0.47 ± 0.15	0.23 ± 0.06	0.42 ± 0.01	0.42 ± 0.01
C18:1ω9	10.59 ± 1.81	6.28 ± 0.75	4.79 ± 0.15	4.53 ± 0.13	12.23 ± 0.93
C18:0	3.4 ± 0.37	4.36 ± 0.36	5.53 ± 0.31	7.53 ± 0.36	2.42 ± 0.21
C19:Cyclo	0.32 ± 0.04	0.42 ± 0.08	0.34 ± 0.02	0.36 ± 0.09	0.26 ± 0.05
C19:0	2.18 ± 0.33	3.98 ± 0.42	3.12 ± 0.48	3.6 ± 0.18	1.6 ± 0.42

Fig. 1

(A)

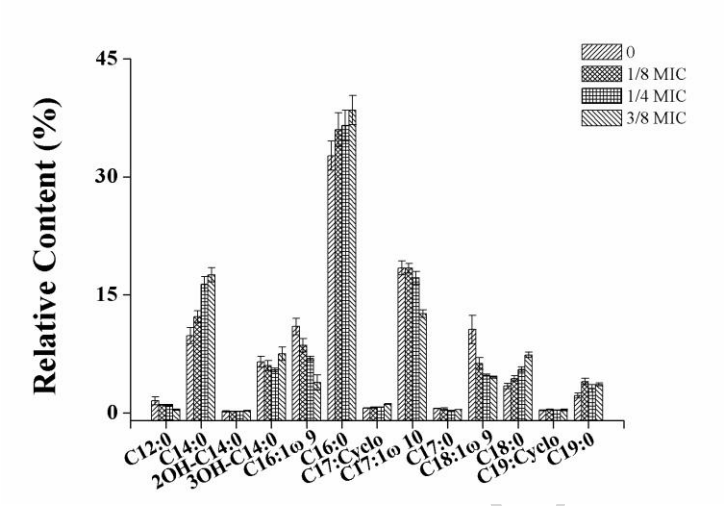

(B)

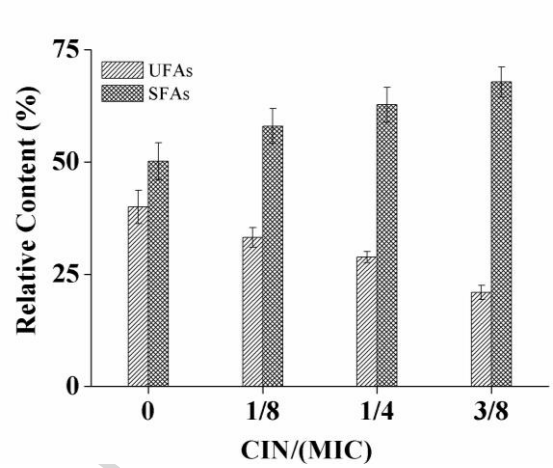

(C)

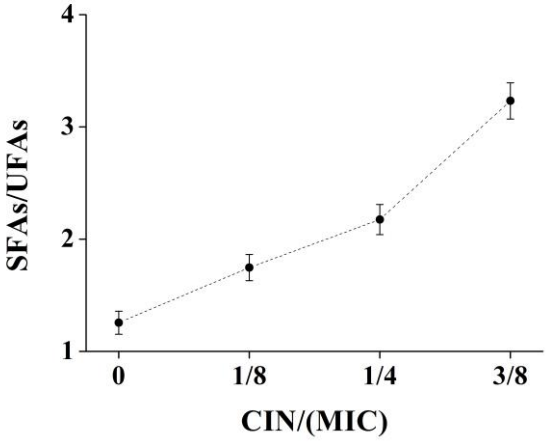

Fig. 2

(A) (B)

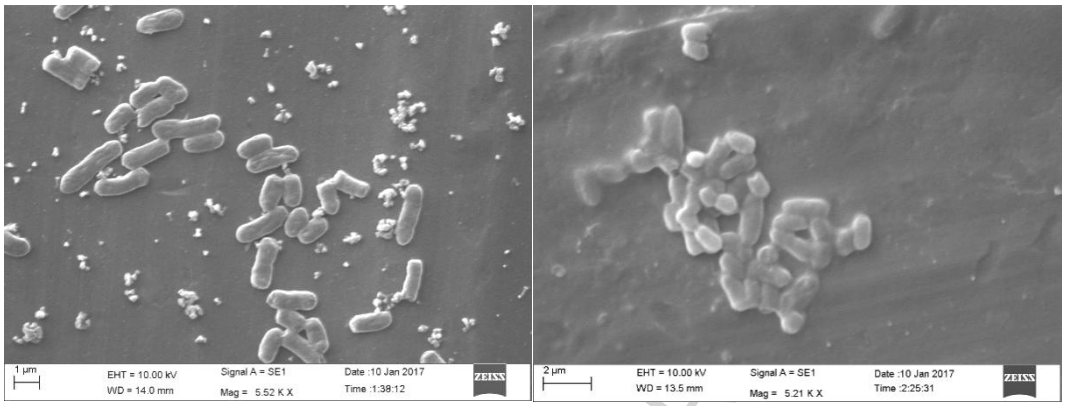

(C) (D)

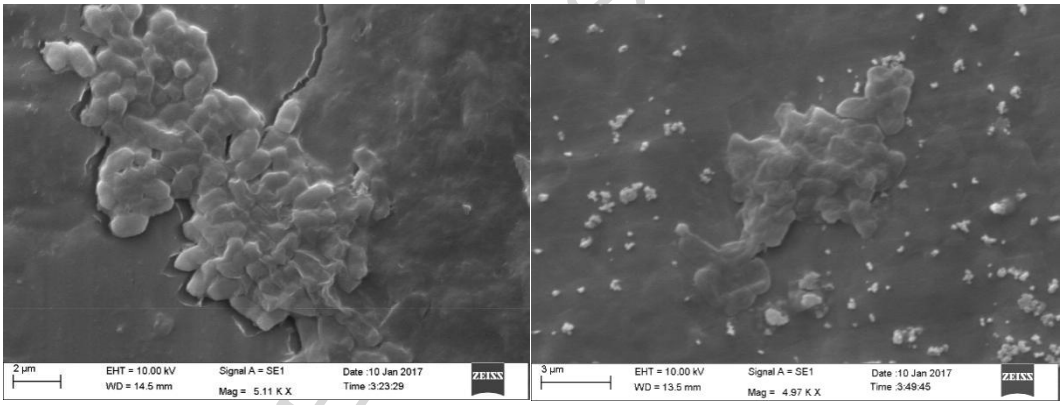

Fig. 3

(A)

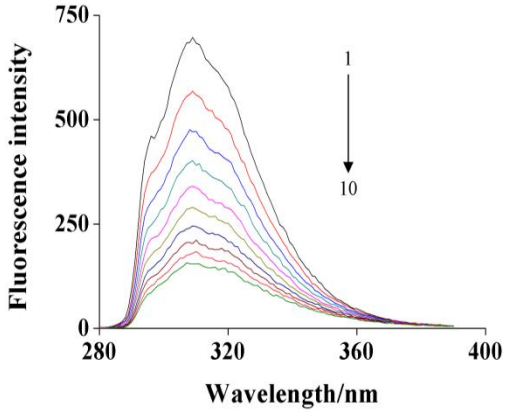

(B)

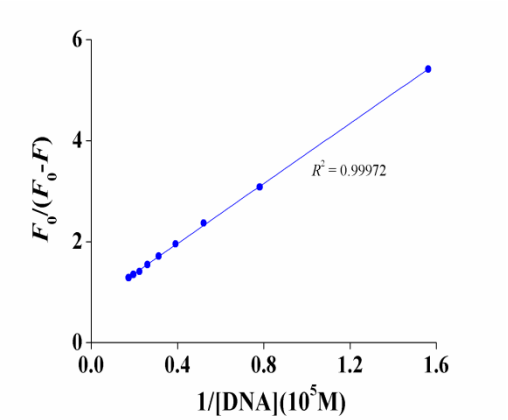

(C)

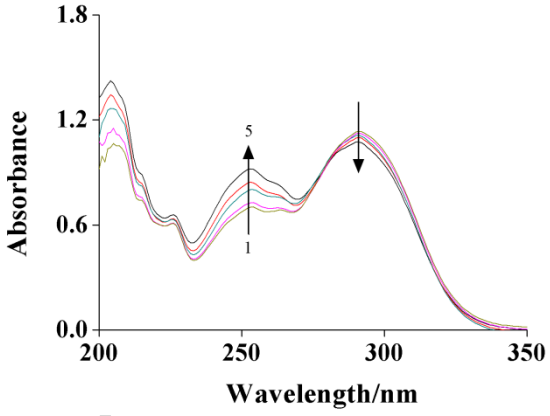

(D)

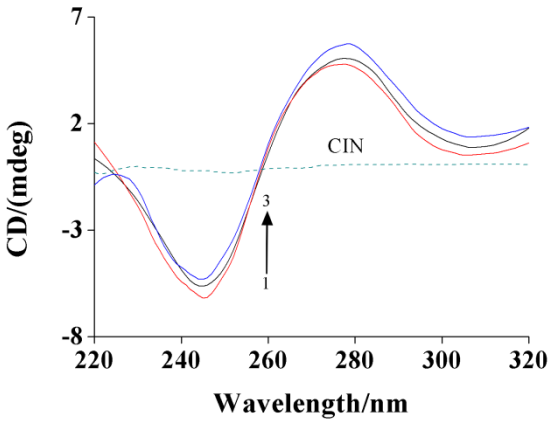

Fig.4

(A)

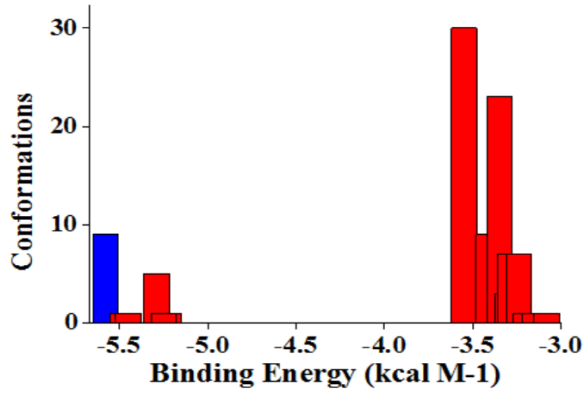

(B)

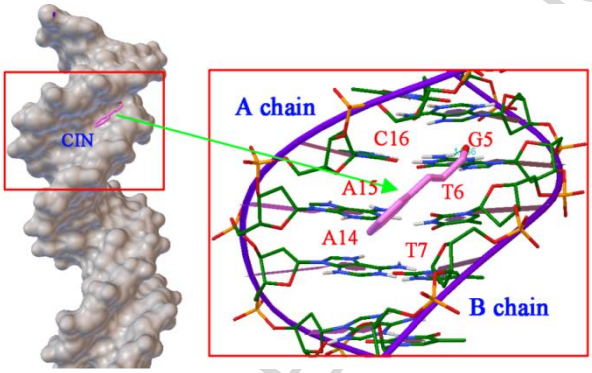

Fig. 5

(A) (B)

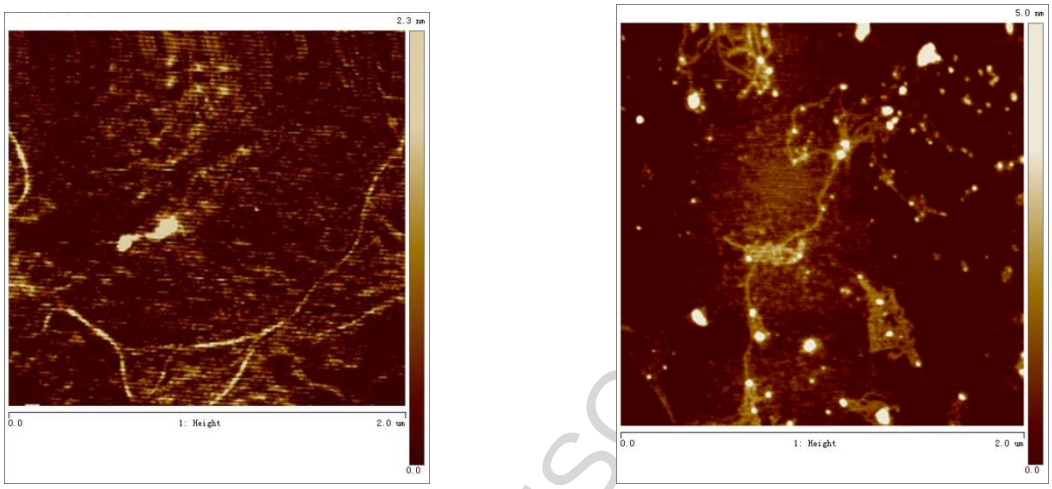

(C) (D)

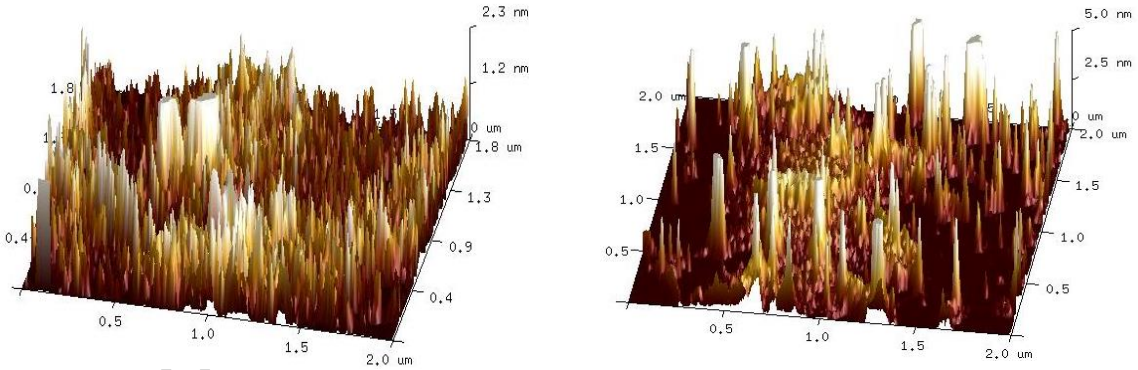

Highlights

> Low levels of cinnamaldehyde induced the alteration of cells membrane fatty acid.

> Binding of cinnamaldehyde to DNA resulted mildly changes in the structure of DNA.

> Cinnamaldehyde changed cell morphology.

> AFM revealed morphological changes of genomic DNA induced by cinnamaldehyde.